

# Pressure-Induced Large Emission Enhancements of Cadmium Selenide Nanocrystals

Guanjun Xiao,<sup>†</sup> Yingnan Wang,<sup>‡</sup> Dong Han,<sup>§</sup> Kexue Li,<sup>§</sup> Xiaolei Feng,<sup>||,⊥</sup> Pengfei Lv,<sup>†</sup> Kai Wang,<sup>†</sup> Lei Liu,<sup>§</sup> Simon A. T. Redfern,<sup>||,⊥</sup> and Bo Zou<sup>\*,†</sup>

<sup>†</sup>State Key Laboratory of Superhard Materials, College of Physics, Jilin University, Changchun 130012, China

<sup>‡</sup>School of Information Science and Technology, Northwest University, Xi'an, 710127, China

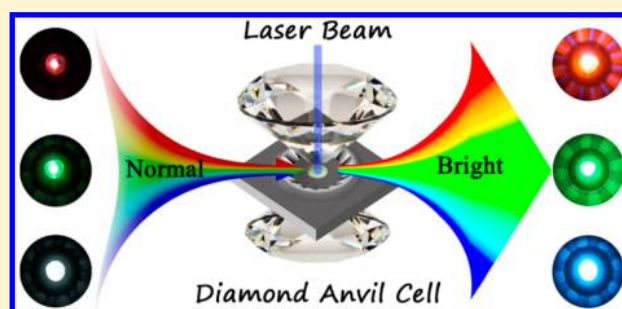
<sup>§</sup>State Key Laboratory of Luminescence and Applications, Changchun Institute of Optics, Fine Mechanics and Physics, Chinese Academy of Sciences, Changchun 130033, China

<sup>||</sup>Center for High Pressure Science and Technology Advanced Research, Shanghai 201203, China

<sup>⊥</sup>Department of Earth Sciences, Downing Street, University of Cambridge, Cambridge, CB2 3EQ, U.K.

## Supporting Information

**ABSTRACT:** Pressure quenching of optical emission largely limits the potential application of many materials in optical pressure-sensing devices, since emission intensity is crucially connected to performance. Boosting visible-light emission at high pressure is, therefore, an important goal. Here, we demonstrate that the emission of CdSe nanocrystals (NCs) can be enhanced by more than an order of magnitude by compression. The brightest emission can be achieved at pressures corresponding to the phase transitions in different sized CdSe NCs. Very bright blue emission can be obtained by exploiting the increase in band gap with increasing pressure. First-principles calculations indicate that the interaction between the capping oleic acid (OA) layer and the CdSe core is strengthened with increased Hirshfeld charge at high pressure. The effective surface reconstruction associated with the removal of surface-related trap states is highly responsible for the pressure-induced emission enhancement of these CdSe NCs. These findings pave the way for designing a stress nanogauge with easy optical readout and provide a route for tuning bright-fluorescence imaging in response to an externally applied pressure.



## INTRODUCTION

Luminescent semiconductor nanocrystals (NCs) hold immense promise in applications such as light-emitting diodes, biomedical labeling, and lasers devices.<sup>1,2</sup> One of the most extensively studied semiconductor NCs, CdSe NCs are of considerable interest in view of their narrow-band and size-dependent photoluminescence (PL), dictated by the quantum confinement effect.<sup>3</sup> It is well established that the PL intensity and wavelength are two key parameters used to assess the performance of optoelectronic devices. To date, considerable efforts have been made to enhance the emission at tunable and controllable wavelengths in CdSe NCs. Several approaches have been taken, including surface passivation with inorganic shells, suppression of nonradiative recombination at low temperature, and introduction of cation disorder.<sup>4–6</sup> Despite significant progress, success in increasing the PL intensity has been limited and there are very few reports of the blue-blind emission. It is increasingly apparent that high pressure may significantly modify the electronic structure, and hence chemical behavior, of compounds. Examples include new and unexpected sodium–chlorine compounds that become stable at high pressure,<sup>7</sup> as well as very many other reports of the use

of pressure to generate novel materials.<sup>8–17</sup> Examples of successful synthesis even extend to high-pressure metastable phases,<sup>18</sup> such as B31-MnS nanomaterials, which are unlikely to be crystallized as bulk counterparts at ambient conditions.<sup>19</sup> Recently, mechanically stable one-dimensional CdSe nanowires were obtained via a high pressure route through the consolidation of spherical CdSe NC arrays.<sup>20</sup> Additionally, obtaining improved performance from nanomaterials at high pressure is important over a wide range of applications. Thus, Tolbert and Alivisatos pioneered the improvement of the high-pressure optical response of organic phosphine capped CdSe NCs.<sup>21</sup> Subsequently, high-pressure optical techniques have been used to determine the band structures and phase stabilities of a number of semiconductor nanomaterials, including Si nanoparticles, MoS<sub>2</sub> nanosheets, InP nanowires, and CsPbBr<sub>3</sub> NCs.<sup>22–28</sup> These materials are, however, plagued by stress-induced PL degradation which frequently dominates at high pressure and limits their potential application as optical pressure-sensing devices.

Received: August 31, 2018

Published: September 28, 2018

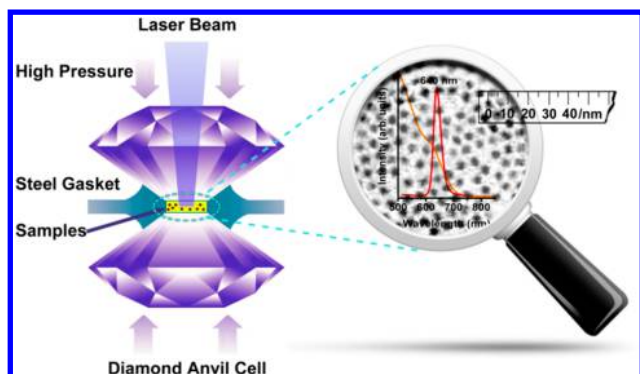


**Figure 1.** Schematic illustration of the DAC apparatus and experimental configuration by enclosing the OA-capped CdSe NCs with an average diameter of 4.8 nm. Inset shows the TEM image of CdSe NCs with the corresponding absorption and PL spectra.

We here demonstrate a pressure-induced emission enhancement (PIEE) of oleic acid (OA) capped CdSe NCs. The maximum PL intensity at high pressure becomes approximately an order of magnitude greater than its original value. Furthermore, very bright blue emission is possible as a result of the band gap blue shift upon increasing pressure. Anomalous pressure anti-quenching of luminescence in CdSe NCs terminated with OA manifests the importance of the interaction between the capping layer and the semiconductor core, especially for the interface energy-level structure. First-principles calculations indicate that the increased Hirshfeld

charge transferred from the OA molecule to CdSe NCs, accompanied by the disappearance of surface-related trap states at high pressure, is the driver for the marked PIEE. Thus, a previously unreported route for tuning bright-fluorescence imaging is proposed, resulting from an externally applied pressure. These processes may find application in a wide range of optical pressure-sensing devices.

## RESULTS AND DISCUSSION

Size-controlled CdSe NCs were synthesized following previously described methods.<sup>29</sup> Quantum confinement of CdSe NCs leads to an increase in band gap with decreasing particle size (Figure S1), which is experimentally expressed as a blue shift in the absorption onset, along with a drastic change of the emission color. High-pressure experiments using a diamond anvil cell (DAC) enclosed the OA-capped CdSe NCs in the sample chamber (Figure 1). Transmission electron microscopy (TEM) of CdSe NCs is shown in the inset of Figure 1, with the corresponding absorption and narrow-band PL spectra. A high-resolution TEM image demonstrates that these NCs exhibit faceted morphology and good crystallinity with well-developed lattice fringes (Figure S2). On increasing pressure the PL spectra of crude CdSe NCs reflect the intrinsic colors which range from red to blue (Figure 2). Intriguingly, a stark PIEE was seen in various CdSe NCs, accompanied by an increase in the energy gap due to the compression of CdSe unit cell parameters.<sup>30</sup> This PIEE was unambiguously confirmed by the pressure-dependent light microscopy images of the interior

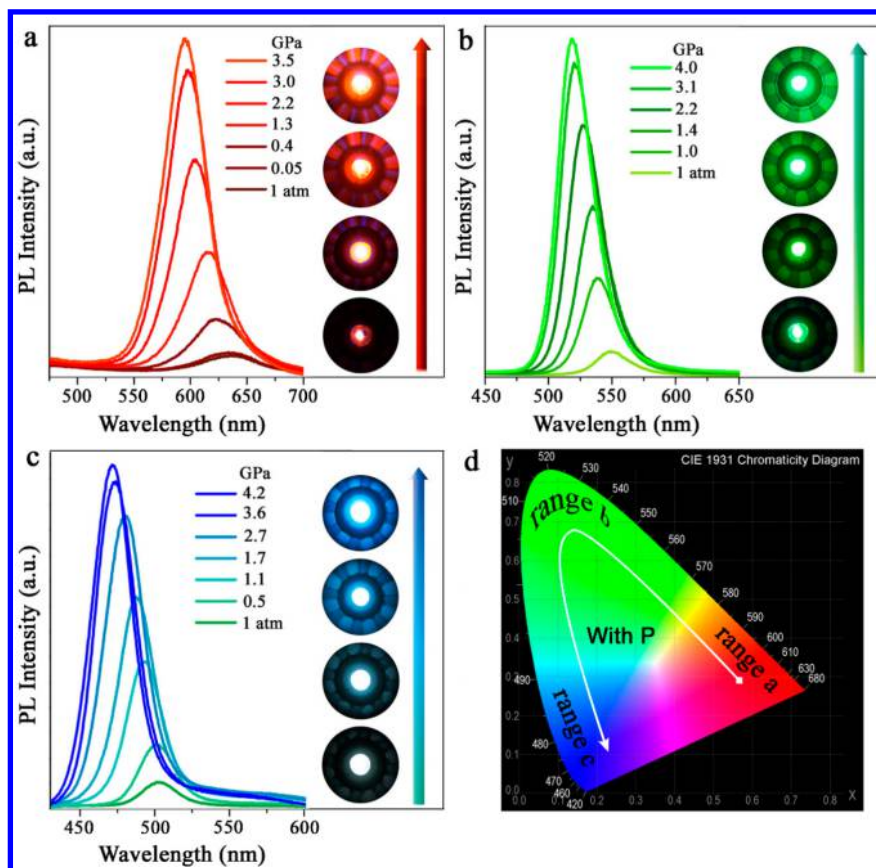


**Figure 2.** High-pressure PL experiments. (A–C) PL spectra of different sized CdSe NCs with increasing pressure, covering the color range from red to blue. Right hand insets in each Figure show micrographs of the DAC interior. (D) Color gamut changes of the different sized CdSe NCs with increasing pressure.

DAC (right panels in Figure 2a–c). An increase in PL intensity of the CdSe NCs is observed with decreasing size and persists at pressures of roughly 3.5, 4.0, and 4.2 GPa. These critical pressures coincide with the reported occurrences of the size-dependent phase transformation of CdSe NCs, from tetrahedral coordination in the wurtzite structure to a denser six-coordinated rocksalt phase.<sup>21,31,32</sup> At higher pressures, the PL intensity of the CdSe NCs gradually decays with increasing pressure before vanishing above ~7.0 GPa, as a featureless emission associated with the indirect band gap in rocksalt CdSe NCs<sup>30</sup> (Figure S3). We find very bright emission across almost the entire visible spectrum under the stimulus of high pressure, applied to a range of differently sized CdSe NCs. Furthermore, the unexpected PIEE persisted over three cycles of pressurization (Figure S4).

In order to determine the origin of the anomalous emission enhancement of the CdSe NCs at high pressure, we systematically investigated the influence of the capping ligands and solvents involved. First, the CdSe NCs were synthesized in the absence of trioctylphosphine oxide, keeping other parameters unchanged (Figure S5). Similar PIEE was observed when the as-prepared crude CdSe NCs were subjected to external pressure, suggesting that trioctylphosphine oxide, as a secondary surfactant ligand, has little effect on the enhanced emission. Second, to exclude the influence of the non-coordinating solvent, octadecene, comparative experiments were conducted using phenyl ether or oleylamine as solvents, respectively. It was found that the emission of the resulting CdSe NCs also exhibited a similar emission enhancement at high pressure (Figure S6a, b). Furthermore, only weak emission enhancement in the mixture of purified CdSe NCs and octadecene occurred at high pressure (Figure S6c), suggesting that the solvents (octadecene, phenyl ether, or oleylamine) are not the cause of PIEE. Third, we substituted oleylamine as the capping ligand in place of trioctylphosphine to synthesize CdSe NCs (details in Materials and Methods in the Supporting Information (SI)). By compressing the crude CdSe NCs prepared in this manner, similar PIEE was found, which rules out trioctylphosphine as the origin of the enhanced emission (Figure S7). Fourthly, taking the coordinated role of OA into account, we synthesized CdSe NCs by adopting the modified method without any fatty acid (see Materials and Methods in the SI). When the crude CdSe NCs obtained in this manner were compressed, no significant emission enhancement was seen, compared to that of OA-capped CdSe NCs (Figure S8). Furthermore, when the excess capping ligand of OA was removed by the purification process, only a weak emission enhancement occurred in CdSe NCs at high pressure, regardless of whether the pressure transmitting medium was present or not (Figure S9). These results indicate that the OA molecules are the dominant control on the strong PIEE of CdSe NCs.

A mixture of purified CdSe NCs and extra OA was loaded into the symmetric DAC apparatus to investigate its PL behavior under high pressure. As expected, significantly stronger PL enhancement occurred, regardless of the dispersion of CdSe NCs in OA (Figure 3). The luminescence changed intuitively from weak pink to bright green. Further compression led to a decrease in the PL intensity of CdSe NCs, until it ultimately disappeared at a pressure of approximately 6.8 GPa, accompanied by a continuous blue shift in the band gap up to ~220 meV (Figure S10). Moreover, *in situ* high-pressure absorption spectra of both crude colloidal

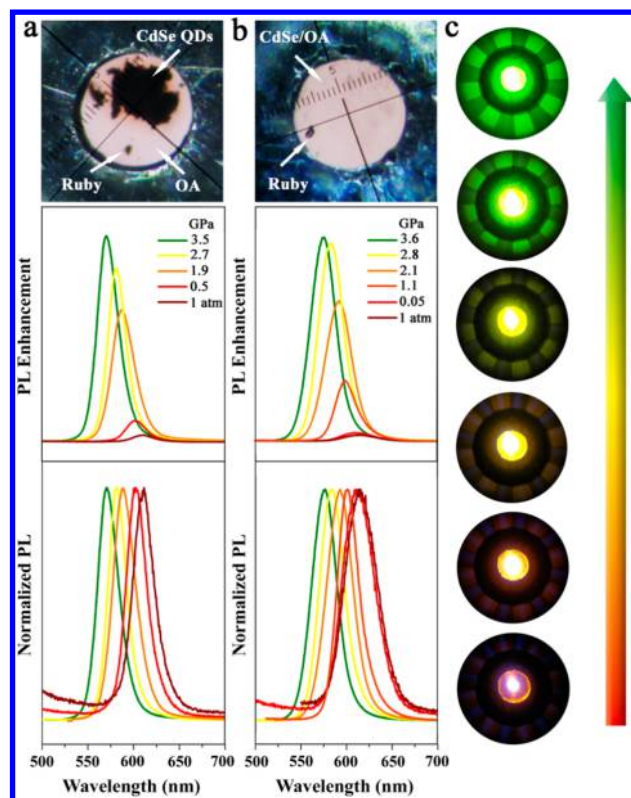


**Figure 3.** Pressure-dependent PL spectra of the mixture of purified CdSe NCs and OA. (A) Undispersed CdSe NCs in OA. (B) Well-dispersed CdSe NCs in OA. The complete behaviors of the pressure-dependent PL spectra are shown in Figure S10. (C) Digital images of color and luminance change with increasing pressure.

CdSe NCs and the hybrid mixture of purified CdSe NCs and OA also exhibited a blue shift associated with tunable pressure-dependent band gaps (Figure S11). Corresponding absorption pressure coefficients are estimated to be about 36.9 and 38.9 meV/GPa, respectively, indicating a strong pressure effect on band gap. The quenched absorption and PL spectra returned to their original peak positions with relatively weak intensities, associated with pressure-induced reversible phase transition of CdSe NCs (Figure S12). Bright luminescence reappeared on decreasing pressure during the quenching process, despite a pressure hysteresis effect. The PL intensity against the pressures for different CdSe NCs systems, as shown in Figure S13, is well-fitted to a Gaussian according to

$$Y = Y_0 + \frac{A}{\sigma\sqrt{2\pi}} e^{-\frac{1}{2}\left(\frac{P-P_c}{\sigma}\right)^2}$$

where  $Y$  is the enhancement factor of the PL intensity at the pressure of  $P$  (GPa), and the parameters  $Y_0$ ,  $A$ ,  $\sigma$ , and  $P_c$  represent the intrinsic constants for the different CdSe NCs systems (Table S1). This correlation facilitates the determination of accurate phase transformation critical pressures by fitting the inflection point of successive PL intensities against pressures.

To gain an insight into the carrier relaxation dynamics of CdSe NCs, we examined their time-resolved PL spectra as a function of pressure. The typical pressure-dependent PL decay curves for crude CdSe NCs and the hybrid mix of well-dispersed CdSe NCs and OA are displayed in Figure 4. At atmospheric pressure, an average PL lifetime of 15 ns is



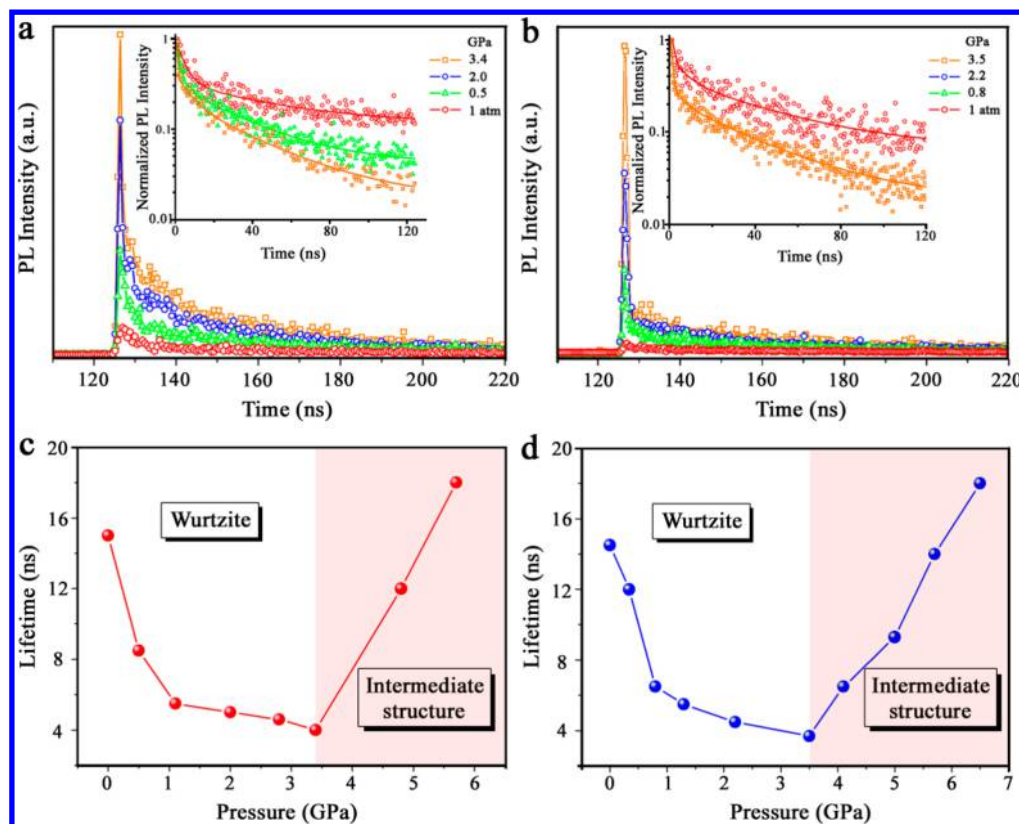


**Figure 4.** Pressure-dependent PL decay curves. (A, C) Crude CdSe colloidal NCs. (B, D) well dispersed CdSe NCs in OA. Therein, the insets in the top panels represent the corresponding normalized PL decay curves fitted with the exponential formula.

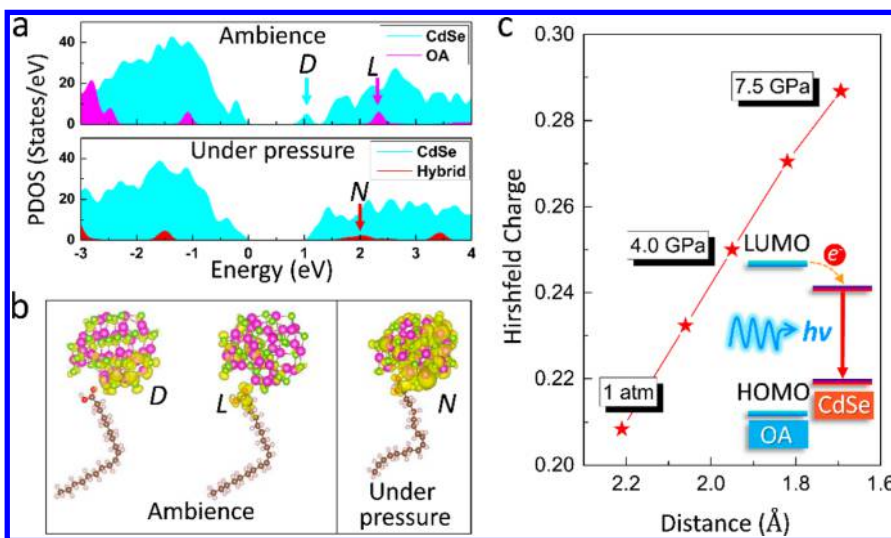


**Figure 5.** First-principles calculations. (A) Partial density of states of CdSe and OA at ambience and high pressure. An energy of 0 eV indicates the position of the Fermi level ( $E_F = 0$  eV). (B) Electron density distributions of the trap states *D*, LUMO level *L* of OA, and new hybridized states *N*, which are labeled in partial density of states. The isosurface of electron distribution is  $0.0005 \text{ e}/\text{\AA}^3$ . Therein, the Cd and Se atoms are denoted as pink and green, respectively, in the ball-and-stick models. The brown chain represents the OA molecule. (C) Hirshfeld charge transferred from OA to CdSe NCs vs the distance between them when the applied pressure was increased to 7.5 GPa in computations.

determined for the crude CdSe NCs by fitting the decay curve (Figure 4a, c). As the pressure gradually increases, the average PL lifetime becomes shorter, implying an increase in the oscillator strength as a result of depressed trap states. To a large extent, this stress-related more rapid decay should contribute to the improvement of the PL intensity with increasing pressure. As soon as the pressure rises to  $\sim 3.4$  GPa,

the average PL lifetime of CdSe NCs reached a minimum of about 4 ns. Upon further compression, the PL lifetime of the CdSe NCs undergoes an apparent increase, indicating a pressure-restrained exciton recombination rate (Figure S14). This observed decay of CdSe emission can be well interpreted by the previous computation of the faceted CdSe NCs.<sup>32</sup> The longer PL lifetime may be attributed to the involvement of the

surface defects in the phase transition process to the indirect band gap of CdSe NCs. This change in decay rate correlates extremely well with that of the PL intensity changes under high pressure. It is noteworthy that, for the mixture of purified CdSe NCs and extra OA, analogous results were also observed (Figure 4b, d).

To further explore the PIEE, we performed first-principles calculations using density-functional theory. A self-healing wurtzite CdSe nanostructured model containing 33 Cd atoms and 33 Se atoms was adopted, in which structural relaxation opens up the energy gap without the aid of passivation or projecting out states.<sup>33</sup> When CdSe NCs and OA molecules coexist, the OA molecules prefer to bond with Cd atoms on the surface of CdSe NCs.<sup>34</sup> The partial density of states indicates that the lowest unoccupied molecular orbital (LUMO) of the OA molecule is located above that of CdSe NCs with surface-related trap states *D* (Figure 5a). The corresponding electron density distribution of the LUMO level *L* of OA and the trap states *D* of CdSe NCs are clearly spatially separated (Figure 5b). This is indicative of the weak interaction between CdSe NCs and the OA molecule at ambient conditions. However, the trap states *D* of CdSe NCs are effectively passivated by external pressure, ultimately vanishing from the energy gap. Concomitantly, the new hybridized states *N* lying above the LUMO level of CdSe NCs appeared owing to the stronger orbital coupling between the OA molecule and CdSe NCs. The electron density of the new hybridized states spread over the CdSe NCs and the OA molecule, rather than distribute locally in either of them. Thus, it can be concluded that the interaction between CdSe NCs and the OA molecule is strengthened with the decreased bonded distance at high pressure. In addition, application of external pressure can break the weak side-to-side bonding of ligand bundles, thus freeing up the ligand molecules and increasing molecular conformational entropy. A previous report demonstrated that the lamellar spacing of OA molecules undergoes a small reducing magnitude upon compression, but the inter-NC distance reduces to a much greater extent.<sup>35</sup> The pronounced difference in compression behaviors will ultimately lead to a further decrease in distance between CdSe NCs and the surface coating of OA molecules at high pressure, which accordingly strengthens the NC–ligand interactions. In this case, the Hirshfeld charge transferred from the OA molecule to the CdSe NCs increased from 0.21 to 0.29, as the bonded distance changed from 2.2 to 1.7 Å (Figure 5c). Note that, over the whole computation in this study, the optimized structure of CdSe still maintained the initial wurtzite configuration without any phase transformation. The exact pressure on the system would be much smaller than our estimation owing to the limitation in theory. On increasing pressure, the surface nonradiative recombination of CdSe NCs is significantly suppressed, as a result of the effective stress-tuned coupling of electronic states.<sup>36,37</sup> Furthermore, the extra excited electrons relax through radiative recombination between the LUMO level and the highest occupied molecular orbital (HOMO) level of CdSe NCs.<sup>38,39</sup> Accordingly, the dominant bulk-related luminescence is enabled by pressure-induced electron transfer, giving rise to the observed PIEE associated with the defects removal by high pressure.

## CONCLUSIONS

In summary, unexpected PIEE is found in OA-capped CdSe NCs. The maximum PL intensity at high pressure reaches an

order of magnitude greater than that of the original at ambient conditions. By combining the pressure-driven band gap broadening and the concomitant boosted intensities, the stark luminescence is easily controlled and encompasses almost the entire visible region. It is noteworthy that very bright blue emission can also be obtained as a result of a blue shift in the band gap with increasing pressure. The improved stability of the PL to pressure quenching, in OA-coated CdSe NCs, points to the importance of the interaction between the capping layer and the semiconductor core. First-principles calculations demonstrate that the increased Hirshfeld charge transferred from the OA molecule to the CdSe NCs under high pressure is responsible for the PIEE in CdSe NCs. These findings provide insights into the mechanisms underlying PIEE and underline its potential application in optical pressure sensors.

## ASSOCIATED CONTENT

### Supporting Information

The Supporting Information is available free of charge on the ACS Publications website at DOI: 10.1021/jacs.8b09416.

Materials and Methods, Comparative high-pressure optical experiments, and low temperature response (PDF)

## AUTHOR INFORMATION

### Corresponding Author

\*zoubo@jlu.edu.cn

### ORCID

Guanjun Xiao: 0000-0002-7013-1378

Kai Wang: 0000-0003-4721-6717

Simon A. T. Redfern: 0000-0001-9513-0147

Bo Zou: 0000-0002-3215-1255

### Notes

The authors declare no competing financial interest.

## ACKNOWLEDGMENTS

The authors acknowledge funding support from the National Key R&D Program of China (No. 2018YFA0305900), the National Natural Science Foundation of China (Nos. 21725304, 11774125, 61525404, 11504368, 11774120, 21673100, and 91227202), the Chang Jiang Scholars Program of China (No. T2016051), Changbai Mountain Scholars Program (No. 2013007), National Defense Science and Technology Key Laboratory Fund (6142A0306010917), Scientific Research Planning Project of the Education Department of Jilin Province (JJKH20180118KJ), and Program for Innovative Research Team (in Science and Technology) in University of Jilin Province. S.A.T.R. acknowledges the support of the NERC grant NE/P019714/1. X.F. is grateful for the support of the China Scholarship Council. Dedicated to Prof. Guangtian Zou on the occasion of 80th birthday.

## REFERENCES

- (1) Dai, X.; Zhang, Z.; Jin, Y.; Niu, Y.; Cao, H.; Liang, X.; Chen, L.; Wang, J.; Peng, X. *Nature* **2014**, *515*, 96.
- (2) Medintz, L. L.; Uyeda, H. T.; Goldman, E. R.; Mattoussi, H. *Nat. Mater.* **2005**, *4*, 435.
- (3) Peng, X.; Manna, L.; Yang, W.; Wickham, J.; Scher, E.; Kadavanich, A.; Alivisatos, A. P. *Nature* **2000**, *404*, 59.
- (4) Xie, R.; Kolb, U.; Li, J.; Basché, T.; Mews, A. *J. Am. Chem. Soc.* **2005**, *127*, 7480.

- (5) Wadhavane, P. D.; Galian, R. E.; Izquierdo, M. A.; Aguilera-Sigalat, J.; Galindo, F.; Schmidt, L.; Burguete, M. I.; Pérez-Prieto, J.; Luis, S. V. *J. Am. Chem. Soc.* **2012**, *134*, 20554.
- (6) Lin, C. C.; Tsai, Y.-T.; Johnston, H. E.; Fang, M.-H.; Yu, F.; Zhou, W.; Whitfield, P.; Li, Y.; Wang, J.; Liu, R.-S.; Attfield, J. P. *J. Am. Chem. Soc.* **2017**, *139*, 11766.
- (7) Zhang, W.; Oganov, A. R.; Goncharov, A. F.; Zhu, Q.; Boulfelfel, S. E.; Lyakhov, A. O.; Stavrou, E.; Somayazulu, M.; Prakapenka, V. B.; Konôpková, Z. *Science* **2013**, *342*, 1502.
- (8) Wang, Z.; Schliehe, C.; Wang, T.; Nagaoka, Y.; Cao, Y. C.; Bassett, W. A.; Wu, H.; Fan, H.; Weller, H. *J. Am. Chem. Soc.* **2011**, *133*, 14484.
- (9) Li, B.; Wen, X.; Li, R.; Wang, Z.; Clem, P. G.; Fan, H. *Nat. Commun.* **2014**, *5*, 4179.
- (10) Wu, H.; Wang, Z.; Fan, H. *J. Am. Chem. Soc.* **2014**, *136*, 7634.
- (11) Wu, H.; Bai, F.; Sun, Z.; Haddad, R. E.; Boye, D. M.; Wang, Z.; Huang, J. Y.; Fan, H. *J. Am. Chem. Soc.* **2010**, *132*, 12826.
- (12) Wu, H.; Bai, F.; Sun, Z.; Haddad, R. E.; Boye, D. M.; Wang, Z.; Fan, H. *Angew. Chem., Int. Ed.* **2010**, *49*, 8431.
- (13) Lü, X.; Hu, Q.; Yang, W.; Bai, L.; Sheng, H.; Wang, L.; Huang, F.; Wen, J.; Miller, D. J.; Zhao, Y. *J. Am. Chem. Soc.* **2013**, *135*, 13947.
- (14) Wang, Y.; Bai, L.; Wen, T.; Yang, L.; Gou, H.; Xiao, Y.; Chow, P.; Pravica, M.; Yang, W.; Zhao, Y. *Angew. Chem., Int. Ed.* **2016**, *55*, 10350.
- (15) Liu, C.; Xiao, G.; Yang, M.; Zou, B.; Zhang, Z.-L.; Pang, D.-W. *Angew. Chem., Int. Ed.* **2018**, *57*, 1893.
- (16) Zhu, H.; Nagaoka, Y.; Hills-Kimball, K.; Tan, R.; Yu, L.; Fang, Y.; Wang, K.; Li, R.; Wang, Z.; Chen, O. *J. Am. Chem. Soc.* **2017**, *139*, 8408.
- (17) Li, Y.; Feng, X.; Liu, H.; Hao, J.; Redfern, S. A. T.; Lei, W.; Liu, D.; Ma, Y. *Nat. Commun.* **2018**, *9*, 722.
- (18) Wang, T.; Li, R.; Quan, Z.; Loc, W. S.; Bassett, W. A.; Xu, H.; Cao, Y. C.; Fang, J.; Wang, Z. *Adv. Mater.* **2015**, *27*, 4544.
- (19) Xiao, G.; Yang, X.; Zhang, X.; Wang, K.; Huang, X.; Ding, Z.; Ma, Y.; Zou, G.; Zou, B. *J. Am. Chem. Soc.* **2015**, *137*, 10297.
- (20) Li, B.; Bian, K.; Zhou, X.; Lu, P.; Liu, S.; Brener, I.; Sinclair, M.; Luk, T.; Schunk, H.; Alarid, L.; Clem, P. G.; Wang, Z.; Fan, H. *Sci. Adv.* **2017**, *3*, e1602916.
- (21) Tolbert, S. H.; Alivisatos, A. *J. Chem. Phys.* **1995**, *102*, 4642.
- (22) Dou, X.; Ding, K.; Jiang, D.; Sun, B. *ACS Nano* **2014**, *8*, 7458.
- (23) Nayak, A. P.; Pandey, T.; Voiry, D.; Liu, J.; Moran, S. T.; Sharma, A.; Tan, C.; Chen, C.-H.; Li, L.-J.; Chhowalla, M.; Lin, J.-F.; Singh, A. K.; Akinwande, D. *Nano Lett.* **2015**, *15*, 346.
- (24) Choi, C. L.; Koski, K. J.; Sivasankar, S.; Alivisatos, A. P. *Nano Lett.* **2009**, *9*, 3544.
- (25) Chauvin, N.; Mavel, A.; Patriarche, G.; Masenelli, B.; Gendry, M.; Machon, D. *Nano Lett.* **2016**, *16*, 2926.
- (26) Hannah, D. C.; Yang, J.; Podsiadlo, P.; Chan, M. K. Y.; Demortière, A.; Gosztola, D. J.; Prakapenka, V. B.; Schatz, G. C.; Kortshagen, U.; Schaller, R. D. *Nano Lett.* **2012**, *12*, 4200.
- (27) Xiao, G.; Cao, Y.; Qi, G.; Wang, L.; Liu, C.; Ma, Z.; Yang, X.; Sui, Y.; Zheng, W.; Zou, B. *J. Am. Chem. Soc.* **2017**, *139*, 10087.
- (28) Nagaoka, Y.; Hills-Kimball, K.; Tan, R.; Li, R.; Wang, Z.; Chen, O. *Adv. Mater.* **2017**, *29*, 1606666.
- (29) Dai, Q.; Li, D.; Chen, H.; Kan, S.; Li, H.; Gao, S.; Hou, Y.; Liu, B.; Zou, G. *J. Phys. Chem. B* **2006**, *110*, 16508.
- (30) Tolbert, S. H.; Herhold, A. B.; Johnson, C. S.; Alivisatos, A. P. *Phys. Rev. Lett.* **1994**, *73*, 3266.
- (31) Tolbert, S. H.; Alivisatos, A. P. *Science* **1994**, *265*, 373.
- (32) Grünwald, M.; Rabani, E.; Dellago, C. *Phys. Rev. Lett.* **2006**, *96*, 255701.
- (33) Puzder, A.; Williamson, A. J.; Gygi, F.; Galli, G. *Phys. Rev. Lett.* **2004**, *92*, 217401.
- (34) Kilina, S.; Ivanov, S.; Tretiak, S. *J. Am. Chem. Soc.* **2009**, *131*, 7717.
- (35) Li, R.; Bian, K.; Hanrath, T.; Bassett, W. A.; Wang, Z. *J. Am. Chem. Soc.* **2014**, *136*, 12047.
- (36) Meulenbergh, R. W.; Strouse, G. F. *Phys. Rev. B: Condens. Matter Mater. Phys.* **2002**, *66*, 035317.
- (37) Wang, Z.; Wen, X.-D.; Hoffmann, R.; Son, J. S.; Li, R.; Fang, C.-C.; Smilgies, D.-M.; Hyeon, T. *Proc. Natl. Acad. Sci. U. S. A.* **2010**, *107*, 17119.
- (38) Wu, Z.; Jin, R. *Nano Lett.* **2010**, *10*, 2568.
- (39) Gan, Z.; Lin, Y.; Luo, L.; Han, G.; Liu, W.; Liu, Z.; Yao, C.; Weng, L.; Liao, L.; Chen, J.; Liu, X.; Luo, Y.; Wang, C.; Wei, S.; Wu, Z. *Angew. Chem., Int. Ed.* **2016**, *55*, 11567.